*American Mineralogist, Volume 63, pages 853–862, 1978*

# Error problems in the two-media method of deriving the optical constants $n$ and $k$ from measured reflectances

PETER G. EMBREY AND ALAN J. CRIDDLE

*Department of Mineralogy, British Museum (Natural History)*
*Cromwell Road, London SW7 5BD, England*

**Abstract**

It has long been recognised that the Fresnel reflectance equations are ill-conditioned for measurements at normal incidence, but the limitations of the two-media method of deriving the refractive index $n$ and the absorption coefficient $k$ have received too little attention. A direct geometrical interpretation of the equations leads to a simplified but general treatment of combinations of measurement errors and their effects. The worst combination of errors results when the measured air reflectance is too high and the oil reflectance is too low, and there is evidence that this is not uncommon in practice. Recommendations are made for a routine procedure in calculations, using a graphical adjunct to computation, which can also be used to select cases where the derivation of constants may confidently be undertaken. The future extension of the two-media method depends on the development of a range of primary reflectance standards, particularly for measurements in oil.

## Introduction

The practical possibility of determining the optical constants of absorbing media from reflectances measured in different surrounding immersion media has been recognised since the pioneering work of Koenigsberger (1913). In addition to the experimental problems of microphotometry, there are limitations inherent in the basic reflectance equations that have received far less attention (Wright, 1919). Recently, Piller and von Gehlen (1964) have discussed the different sources of error, and have calculated the effects of given reflectance errors on derived values of the optical constants, but their treatment of the latter lacked generality.

### *The reflectance equations*

The basic relations between reflectances measured at normal incidence and the optical constants are:

$$R = \{(n-1)^2 + k^2\}/\{(n+1)^2 + k^2\} \qquad (1)$$

$$^{\text{im}}R = \{(n-N)^2 + k^2\}/\{(n+N)^2 + k^2\} \qquad (2)$$

where $n$ is the refractive index and $k$ the absorption coefficient of the absorbing medium, $R$ the reflectance in air, and $^{\text{im}}R$ the reflectance in an immersion oil of refractive index $N$. The symbols $R$ and $^{\text{im}}R$ for the two-media reflectances are recommended by the Commission on Ore Microscopy of the IMA. Although these relations are generally known as the Fresnel equations, they appear to have been first derived in this form by Drude (1890) and later used by Koenigsberger (1913).

Equation (2) is readily rearranged to the forms

$$n^2 + k^2 - 2nN\left(\frac{1 + {}^{\text{im}}R}{1 - {}^{\text{im}}R}\right) + N^2 = 0 \qquad (2a)$$

and

$$\left\{n - N\left(\frac{1 + {}^{\text{im}}R}{1 - {}^{\text{im}}R}\right)\right\}^2 + k^2 = \frac{4N^2\,{}^{\text{im}}R}{(1 - {}^{\text{im}}R)^2} \qquad (2b)$$

In these forms they are immediately recognisable as the equations of circles with centres lying on the $n$-axis. The equations for the air reflectances are obtained by substituting $R$ for $^{\text{im}}R$, with $N = 1$.

Holl (1967) has observed that the reflectance equations for all angles of incidence, and not merely those for normal incidence, may be represented by families of circles. Comparison of equation (2a) with the more general form $x^2 + y^2 - 2gx + c = 0$ (Coxeter, 1969) shows that these families of circles are *coaxal sets*, or *pencils*; the points $(\pm 1,0)$ and $(\pm N,0)$ on the $n$-axis are the *limiting points* of the air and oil sets.

If we define $a$ and $h$ as the distances of the centres of air and oil reflectance curves, respectively, from

0003-004X/78/0910-0853$02.00

the origin, we have [from equation (2b)]

$$a = \left(\frac{1+R}{1-R}\right) \quad \text{and} \quad h = N\left(\frac{1+{}^{\text{im}}R}{1-{}^{\text{im}}R}\right) \qquad (3)$$

and the radii of the curves are given by

$$\text{radius (air)} = \frac{2\sqrt{R}}{(1-R)} \quad \text{and}$$

$$\text{radius (oil)} = \frac{2N\sqrt{{}^{\text{im}}R}}{(1-{}^{\text{im}}R)} \qquad (4)$$

Solving equations (1) and (2) to obtain $n$ and $k$ from measured reflectances, we obtain the equations

$$n(\text{calc}) = \frac{\frac{1}{2}(N^2-1)}{\frac{N(1+{}^{\text{im}}R)}{(1-{}^{\text{im}}R)} - \left(\frac{1+R}{1-R}\right)} \qquad (5)$$

$$k(\text{calc})^2 = \frac{R(n_{(\text{calc})}+1)^2 - (n_{(\text{calc})}-1)^2}{(1-R)} \qquad (6)$$

These are sometimes known as the Koenigsberger equations. The denominator of equation (5) is the distance between the centres of an oil and an air reflectance curve, so we may simplify it [from equation (3)] to the form

$$n(\text{calc}) = \tfrac{1}{2}(N^2-1)/(h-a) \qquad (5a)$$

and by substitution in equation (6) we obtain

$$k(\text{calc})^2 = \{(N^2a-h)/(h-a)\} - \{\tfrac{1}{2}(N^2-1)/(h-a)\}^2 \qquad (6a)$$

Pepperhoff (1965) has derived comparable equations containing both the positions of the centres and the lengths of the radii of the curves, but they have no additional advantage for our immediate purpose.

**Graphical representations of the reflectance equations**

The first graphical representations of the reflectance equations were published by Wright (1919), who plotted curves of constant absorption index (kappa) on $R/n$ coordinate axes and curves of constant reflectance on $n/\kappa$ (kappa) axes. Ponomareva (1958) plotted curves of constant $n$ and $\kappa$ (kappa), using $R/{}^{\text{im}}R$ axes; Piller and von Gehlen (1964) independently plotted a similar diagram for $n$ and $k$ (kay) contours, and from the shape of the $k = 0$ curve referred to it as a cigar. Pepperhoff (1965) published curves of constant $R$ and ${}^{\text{im}}R$ on $n/k$ (kay) coordinate axes, and appears to have been the first to recognise them explicitly as circular arcs (when the units are equal on the two axes). We shall refer to the latter types of representation as the $n/k$ diagram and the $R/{}^{\text{im}}R$ cigar diagram. Charts of the iso-reflectance curves have been used to obtain a graphical solution of the reflectance equations for $n$ and $k$, and Galopin and Henry (1972, p. 177) have remarked that a poor 'fix' results when the air and oil curves intersect in a shallow angle (Fig. 1).

*The n/k diagram*

Although the reflectance equations represent circles, we are only concerned with semicircles in the first quadrant where $n$ and $k$ are both positive and real. Circles in the second and third quadrants, with $n$ negative, correspond to imaginary reflectances (greater than 100 percent).

For any given pair of values of $n$ and $k$, a point P is fixed which is the intersection of a unique pair of iso-reflectance curves $R$ and ${}^{\text{im}}R$ for a given value of $N$; but the converse is not generally true. For a given value of $R$, only a limited range of values of ${}^{\text{im}}R$ will produce an intersection, and *vice versa*. Experimental data consist of pairs of $R$ and ${}^{\text{im}}R$ values, which are subject to error; if the corresponding curves do not intersect, the solution for $n$ and $k$ will be imaginary. Even when the corresponding curves do intersect, to give real values of $n$ and $k$, these values will be in error.

In Figure 1 it can be seen that the intersection angle of a pair of iso-reflectance curves, and the angular position of the intersection relative to each curve, may readily be calculated from the reflectance values which define the centres and radii of the curves. The loci of these angles radiate from the limiting points of the reflectance curves, and are shown for a few values in Figure 2. Comparison of these loci with the computed error curves of Piller and von Gehlen (1964, p. 880) suggests that a 5° intersection angle is near to the minimum value for the confident derivation of $n$ and $k$, with currently attainable accuracy in the measurement of reflectances, and we can see the range of values of these constants that lie within that contour.

In Figure 3 we have drawn the intersection of two reflectance curves, and the region within which a derived point P′($n'$, $k'$) must lie when the measured reflectances are in error on either side of the true values. This diagram, with an acute angle of intersection, is generally applicable because the region within which the intersection is obtuse is very small (Fig. 2). Piller and von Gehlen (1964, Table 2) listed and considered eight principal permutations of possible reflectance errors, which are more clearly seen in our diagram.

Three important conclusions may be drawn from an inspection of Figure 3: the relative elongation of

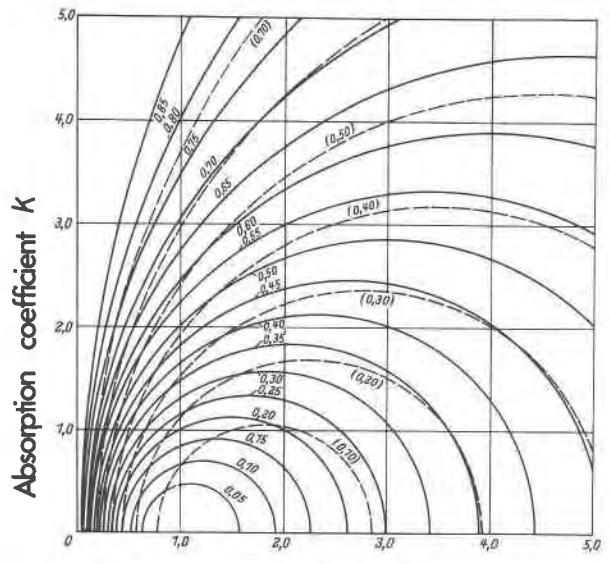


Fig. 1. The relations between the reflectance curves for air (solid) and oil (dashed) and the optical constants $n$ and $k$ (copied from Pepperhoff, 1965, p. 943, Fig. 1). See also Fig. 3. Reflectances are shown as decimal fractions, not as percentages.

the region of resultant error increases as the angle of intersection decreases; error combinations that result in a displacement of the curves relative to each other have the most serious effects on derived values of $n$ and $k$; and, particularly for these largest resultant errors, the distribution of error between $n$ and $k$ depends on the position of the intersection on the reflectance curve of smaller radius (usually that of $^{\text{im}}R$).

The $n/k$ diagram is very useful for qualitative prediction, as the following examples show, but the $R/^{\text{im}}R$ cigar diagram is better for quantitative use. Experimental points taken from von Gehlen and Piller's work on covelline (1964) and on hexagonal pyrrhotine (1965) may be plotted on Figure 2. The point for covelline lies near the 60° intersection contour, where the error region is small (Fig. 3); resultant errors in $n$ and $k$ are thus small, despite the relatively large errors in measuring low reflectances. The pyrrhotine point lies on the curve of $\beta = 90°$, which accounts for the authors' observation that $n$ was much more liable to error than $k$.

### *The $R/^{\text{im}}R$ cigar diagram*

The principal features of the $R/^{\text{im}}R$ cigar diagram are shown in Figure 4. Contours of constant absorption are closed curves radiating from the point ($R = {}^{\text{im}}R = 100$ percent), and lie wholly within the cigar boundary, $k = 0$. Contours of constant absorption coefficient (kay) are displaced to the low-$^{\text{im}}R$ side of the diagram, whereas those of constant absorption index (kappa) are symmetrical about the diagonal $R = {}^{\text{im}}R$ (Ponomareva, 1958). The region inside the cigar is the field of real intersections of the reflectance curves and of real values of $n$ and $k$; the region outside is the imaginary field. Curves of constant $n$ also radiate from ($R = {}^{\text{im}}R = 100$ percent), but they cut the cigar; the portions of the $n$-curves outside the cigar correspond to solutions of equation (5), but have no physical meaning. The curve labelled $n = \pm\infty$ marks the discontinuity beyond which $n$(calc) is negative. Contours of constant intersection angle may also be drawn on this diagram, and are symmetrical about the diagonal line, radiating from and joining the points where the cigar touches the coordinate axes. The 90° contour is an almost straight line between these points and, as in the $n/k$ diagram, encloses a very small region of obtuse intersection angles (*cf.* Fig. 2).

The cigar diagram may be used for the direct determination of $n$ and $k$ from measured reflectances, provided that it has been drawn for the appropriate value of $N$, and for this reason equations for its construction are given in the Appendix. Because the $n$ and $k$ contours are badly crowded at higher reflectances

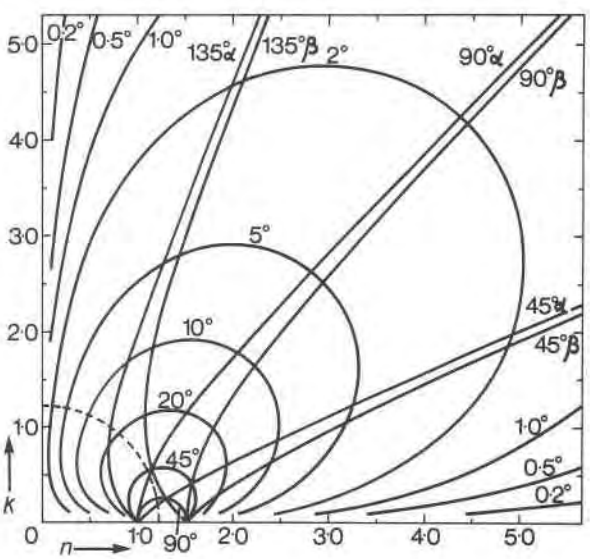


Fig. 2. Contours of constant intersection angle of the reflectance curves for air and oil ($N = 1.515$), and of the angular positions of the intersection on the two curves, $\alpha$ (air) and $\beta$ (oil). The intersection contours should all meet at $n = 1$ and $n = N$. The dashed quarter-circle is the locus of intersections of curves for which $R = {}^{\text{im}}R$; the equation is $n^2 + k^2 = N$. The locus of intersections of curves of equal radius lies between the curves $\alpha = 90°$ and $\beta = 90°$, but is not shown.

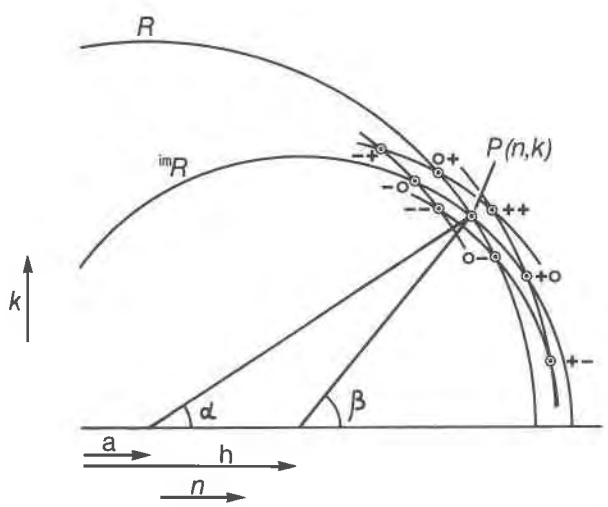


Fig. 3. The position of a point $P(n,k)$ at the intersection of the true reflectance curves $R$ and $^{im}R$, and its angular position on the curves ($\alpha$ and $\beta$). The intersection angle is the (acute) angle $\beta - \alpha$, and $a$ and $h$ are the distances of the centres of the true curves from the origin [see text, equation (3)]. A derived point $P'(n',k')$ lies in the region bounded by arcs of curves for which the measured reflectances are in error; limiting points of this region are labelled (+o) and so on (*i.e.* $R$ too high, $^{im}R$ no error, *etc.*).

near the $k = 0$ boundary envelope, an inevitable consequence of the arithmetical sensitivity of the reflectance equations in this region, it is advantageous to draw a small area to an enlarged scale.

*Graphical demonstration of errors in derived n and k values*

Figure 5 shows an enlarged area of the cigar diagram in the immediate vicinity of points A (53.5 percent $R$, 40.5 percent $^{im}R$) and B (54.5 percent $R$, 39.0 percent $^{im}R$), which we may take as measured values for pyrite, with $N = 1.515$. Let us also suppose that A ($n$ 2.34, $k$ 3.00) is the 'true' point, without error of measurement; in practice, however, we would have no means of knowing this. Errors of +0.5 percent in $R$, and −1.0 percent in $^{im}R$, take us to A′($n$ 4.45, $k$ 3.00); 0.5 percent more in each, in the same directions, bring us to B ($n$ 11.44, $k$ 7.36$i$) which is clearly in the imaginary field. We thus see the rapid increase in the rate of change as errors take the point towards and across the $k = 0$ boundary, and the slow initial change in $k$ on passing through $\beta = 90°$ (*cf.* Fig. 2). These extreme changes in $n$ and $k$ result more from the signs of the errors in measurement than from the size of those errors. Different combinations of the signs, with the sizes of the errors remaining the same, would have produced the points B′($n$ 1.30, $k$ 2.38), C ($n$ 2.68, $k$ 3.00), or D ($n$ 2.07, $k$ 2.96) in Figure 5. Errors of the same sign, and of roughly the same magnitude, displace the true point in nearly the same direction as the run of the contours with little change in $n$ and $k$, as we have already seen from Figure 3.

The computed value of $n$, although a real number for the point B in the imaginary field, is demonstrably as false as that for $k$ (which is complex); the maximum values of $n$, for a real point lying close to the $k = 0$ contour, are near 6.6 (as shown on the diagram).

*A variant of the $R/^{im}R$ cigar diagram*

The basic cigar diagram may be projected in other ways, so that the crowding of the contours is reduced by selective distortion. The most obvious method, which we have drawn but not reproduced in this paper, is to expand the cigar while retaining its length. Another method is to project the lower $k = 0$ contour so that it is a horizontal straight line (Fig. 6);

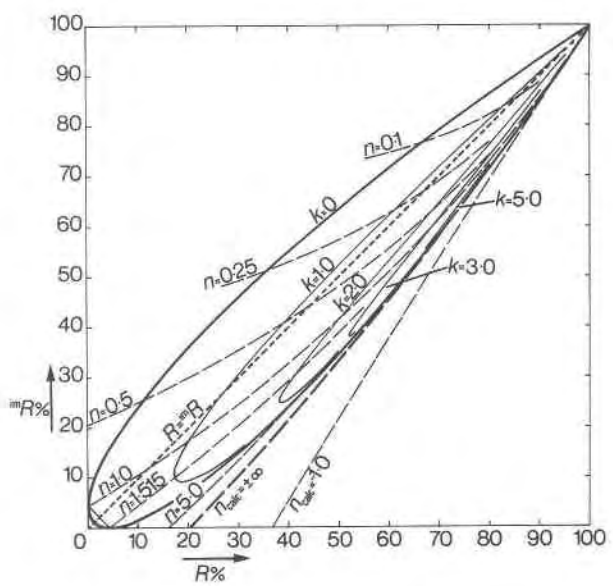


Fig. 4. The $R/^{im}R$ cigar diagram (drawn for $N = 1.515$). The field of real values of $n$ and $k$ (absorption coefficient) lies inside the $k = 0$ contour. Above the cigar, and between it and the curve $n$(calc) = $\pm\infty$, $k$(calc) is complex and $n$(calc) real but false; below the curve $n$(calc) = $\pm\infty$, $k$(calc) is complex and $n$(calc) negative. The short line joining the points where the cigar touches the axes (bottom left) is the 90° intersection contour, the only one shown; the small region of obtuse intersections lies between it and the origin inside the cigar, and contours of acute intersections lie in the remainder of the cigar. The locus of intersections between reflectance curves of equal radius (not drawn) joins the 'blunt ends' of the $k$ contours; the curves $\alpha = 90°$ and $\beta = 90°$ lie on either side of it (*cf.* Fig. 2).

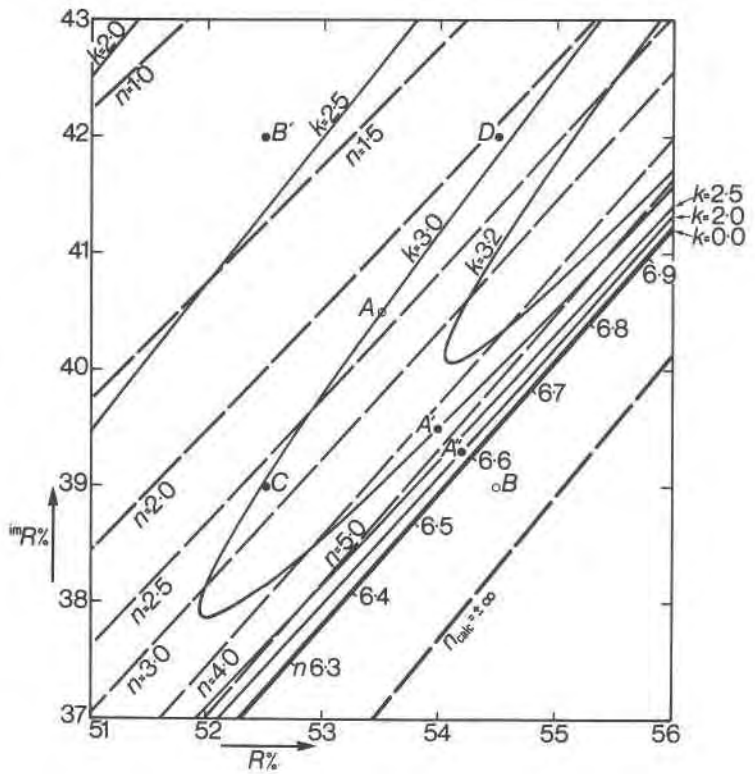


Fig. 5. An enlarged portion of the $R/^{im}R$ cigar diagram ($N = 1.515$). The points $A$ and $B$ represent measured values for pyrite, and $A$ is assumed to be near the true value. $B'$, $C$, and $D$ are points with the same size errors as $B$, but of different sign combinations; $A'$ and $A''$ lie between $A$ and $B$, with smaller errors than $B$ (see text). Intersections of $n$ contours with $k = 0$ are indicated by the value of $n$.

the abscissa is $R$, and the ordinate is the distance of a point from the outer cigar, measured in units of the oil reflectance $^{im}R$. We have selected this variant projection because we found that, when we plotted a large number of measured points on the cigar diagram, a majority lay close to the edge of the cigar; this observation seemed to be best demonstrated by reference to a straight line. The diagram is not suitable for the direct demonstration of the effects of measurement errors, because although errors in $^{im}R$ cause a simple vertical displacement of a point, errors in $R$ affect both coordinates.

## Reflectance errors and their causes

The reflectance data plotted in Figure 6 are taken from the IMA/COM Data File 1977, and are the 194 data points for which there are both air and oil reflectances at 589 nm. The file did not contain derived values of $n$ and $k$, a COM policy decision taken because an investigation is to be made of the accuracy of microphotometric reflectance measurements. It is not at present possible to assess the accuracy of those points lying in the real field, but nearly a quarter of the total lie in the imaginary field and are thus obviously wrong. We have seen from Figure 5 that although positive errors in $R$ alone, or negative errors in $^{im}R$ alone, are capable of putting a point in the (lower) imaginary field, much smaller errors in combination can achieve the same result.

### *The nature of reflectance errors*

The causes of errors in reflectance measurements under the microscope have been considered by Piller and von Gehlen (1964), who divided them into those arising in the equipment and those arising in the specimen itself. Another classification of errors may be made, into random and systematic. We shall not attempt a complete listing of all possible sources of error, of which the most important appear to be:

*Random errors.* Instability of the photometric optical train; instability of the light source and monochromator; inhomogeneity of the reflectance standard; and focussing errors (which may also be systematic for a particular observer).

*Systematic errors.* The nature of the polished surface (which may also be random if the polishing or

cleaning routine is variable); the accuracy of glare and other allied corrections; and the accuracy of the reflectance standard(s).

Modern instruments have been developed to the stage where reflectance measurements are highly repeatable and, if care is taken, reproducible on the same instrument. Considerable trouble is taken by some authors (*e.g.*, Lopez-Soler and Bosch-Figueroa, 1970) to reduce random error by repeated measurement, but it is possible to be too careful over random errors if real systematic errors remain neglected.

The errors recognisable from Figure 6 are, for the most part, too large to be attributable to random causes; we must look elsewhere, and the first objects of our attention must be the reflectance standards.

*Reflectance standards*

"The procurement of material standards of suitable quality is a major limitation of the art" (Clarke, 1972) and considerable efforts have been made in this direction (Hallimond, 1970, p. 152; Galopin and Henry, 1972, p. 159 *et seq.*). Apart from having the necessary physical properties, the materials chosen must be sufficiently large and homogeneous for primary calibration in a standards laboratory; an area of about 1 cm² is often considered adequate, although the National Physical Laboratory prefer 25 cm² for the most accurate work (Clarke, 1972). These requirements, size in particular, have greatly reduced the number of materials available, and Piller (1974; 1977) lists three that are approved by the Commission on Ore Microscopy: neutral glass; single-crystal silicon carbide; and homogeneous mix-crystal tungsten titanium carbide. The crystals available of the last of these are too small for the most accurate primary calibration. Piller (1977) has also recommended liquid surfaces as reference standards in the ultra-violet or near infra-red.

There is a large gap in reflectance in air between SiC (20 percent) and (W,Ti)C (47 percent), and there are as yet no accepted air standards for higher reflectances; but the position is much worse for oil reflectance standards. At present these are all derivative standards, calibrated indirectly by computation from the air reflectance and the refractive index of the oil (Piller, 1974, p. 38; 1977, p. 126) for silicon carbide, assuming zero absorption, and higher reflectances are measured under the microscope by extrapolation from this. There is thus an urgent need for primary standards for reflectances measured in oil; the state of the art has not yet caught up with experimental requirements, and to say this is no criticism of the careful development work that has already been done.

*Measurement errors: conclusions*

Corrections for glare in the optical system are made nowadays as a matter of routine, following the work of Piller (1967) and earlier authors, and these are different for measurements in oil from those made in air. These corrections, however carefully they are calculated, can only be tested for accuracy by actual comparison between two or more primary standards of differing reflectance.

Of the many errors that can adversely affect the two-media derivation of the optical constants, leaving aside those cases where the properties of the surface layer are different from those of the substrate, we conclude that the most serious probably lie in the standards for oil reflectance measurement, due to their current lack of primary calibration and the large extrapolations required from the oil reflectance of silicon carbide ($^{im}R$ about 7 percent). A potential source of additional error in the oil reflectance lies in the oil itself: if the oil used for the measurements is different from that used for the calibration calculations, the values of $^{im}R$ for the standard will be wrong unless recomputed for the new oil. Errors in the measurement of air reflectances, as we have seen, are less likely to be serious.

Unfortunately, we do not yet have the means to test our hypothesis; but we suggest that reflectance measurements may well tend to be in error in the worst possible directions: air high, oil low.

*Immersion oil and accuracy*

It is easily shown that small errors in the refractive index of the immersion oil have little effect compared with those in reflectance. Much larger errors may be caused by the presence of suspended dust or air bubbles. Use of a different oil, with a higher refractive index, increases the spacing of the $n$ and $k$ contours on the cigar diagram and enlarges the area of the $n/k$ diagram enclosed by a given intersection angle contour. The improvement is small, however, for any oil that might be used in practice: if $N$ is 1.70, for example, the 5° contour touches $n = 3.9$ compared with 3.3 when $N = 1.515$ (Fig. 2).

## Deriving the optical constants

The most direct method of deriving the optical constants $n$ and $k$ is by calculation, using the Koenigsberger equations (5) and (6). Desk and pocket programmable calculators have made the use of

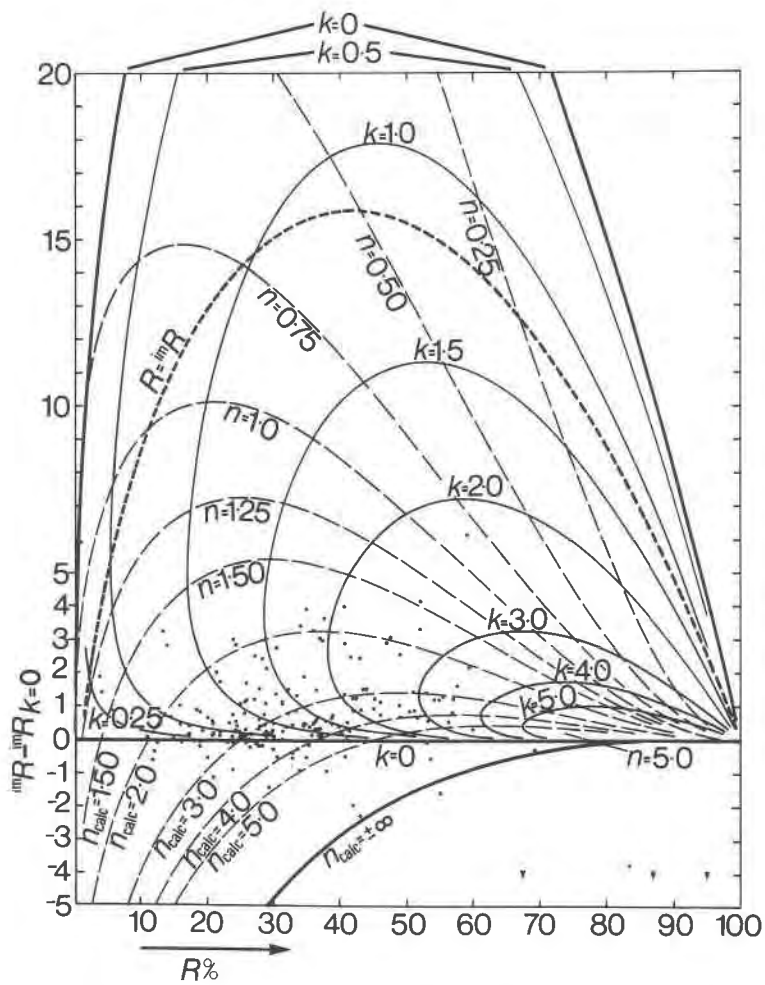


Fig. 6. Variant of the cigar diagram (drawn for $N = 1.515$). The lower part of the $k = 0$ curve is the horizontal straight line from the origin, and the locus of $R = {}^{\text{im}}R$ is the dashed curve (*cf.* Fig. 4). Horizontal units are in $R$ percent; vertical units in ${}^{\text{im}}R$ percent above the $k = 0$ boundary, *i.e* ${}^{\text{im}}R_{n,k} - {}^{\text{im}}R_{k=0}$, and all points below $k = 0$ are in the imaginary field. All $k$ contours are terminated 0.1 percent above the $k = 0$ datum. The plotted points are for 194 pairs of air and oil reflectances at 589 nm, and are taken from the IMA/COM Data File 1977.

nomograms (Volynskii and Yasnopol'skii, 1959) and printed reflectance curves (Pepperhoff, 1965) obsolete; these, in any case, needed ideally to be constructed individually for each value of the refractive index of the immersion oil. The cigar diagram is the easiest of the graphical methods to use, but does not yet appear to have been recommended. This is probably because the whole diagram is tedious and difficult to draw by hand for closely spaced intervals of $n$ and $k$. A small portion of the diagram, however, is an invaluable adjunct to calculation since it also shows clearly and directly the effects of measurement errors.

*Calculation of errors in n and k*

Piller and von Gehlen (1964, p. 881) have stressed that a discussion of errors should accompany all published reflectance measurements, especially when $n$ and $k$ are derived from them, but they did not recommend any guidelines for such discussions.

It is tempting to use the differential calculus to obtain rates of change of the optical constants for changes in the reflectances, and this has been done (Koenigsberger, 1913; Vierne and Brunel, 1977), but a simple approach is only valid when the rates of change are small and nearly steady. In the neighbourhood of the $k = 0$ boundary, however, where $k$ is small in relation to $n$, the rates of change of both $n$ and $k$ accelerate rapidly and it becomes necessary to use Maclaurin's theorem to incorporate second- and higher-order differentials into the calculation. In theory there is no objection to this method of procedure, but in practice it is a cumbersome waste of elegance

because we do not know the probable size of our reflectance errors sufficiently accurately. It would be a different matter if we had only the small random errors to consider, but the larger systematic errors invalidate this approach.

It is far easier, and more realistic, to proceed by applying probable errors to our measured reflectances, calculating their effects from the Koenigsberger equations, and appending a diagram such as that of Figure 5 but with an error circle or ellipse drawn round each measured point. It should also be apparent that the errors in $n$ and $k$ should be expressed in the form $n + x - y$, and not $n \pm z$, because although the reflectance errors may be symmetrical the effects on $n$ and $k$ almost certainly are not.

The $n/k$ contour diagram (Fig. 2) is useful, both as a guide to the expected distribution of errors before the detailed calculations are made and for plotting the $n/k$ points, to indicate the change in the errors at each wavelength in a spectral run. If a computer or programmable calculator is used in the calculations, it is easy to calculate the angles $\alpha$, $\beta$, and the intersection angle as part of the routine. It is also desirable to calculate the position of the point in relation to the $k = 0$ curve, since this gives an immediate warning if the point is so close that it cannot be distinguished (within the limits of error) from a point on the boundary. For this purpose, we may use the following equations obtained from that for the general $k$-contour (see Appendix):

$$h = \tfrac{1}{2}a(N^2 + 1) - \tfrac{1}{2}(N^2 - 1)\sqrt{(a^2 - 1)} \qquad (7a)$$

$$a = \tfrac{1}{2}h(N^2 + 1) + \tfrac{1}{2}(N^2 - 1)\sqrt{(h^2 - 1)} \qquad (7b)$$

where $a$ and $h$ are related to the reflectances $R$ and ${}^{\mathrm{im}}R$ by equations (3).

This last calculation is more important than appears at first sight, as an example shows. The point A″ (Fig. 5) has $R$ 54.20 percent, ${}^{\mathrm{im}}R$ 39.30 percent, for which $n = 5.890$, $k = 1.992$, but the intersection angle is only 1.25°. From equations (7a) and (7b) we find that if $R$ is constant, ${}^{\mathrm{im}}R$ at the $k = 0$ boundary is 39.159 percent; if ${}^{\mathrm{im}}R$ is constant, $R$ at the boundary is 54.325 percent. In other words, changes of only (+) 0.23 percent (relative) in $R$, or (−)0.36 percent in ${}^{\mathrm{im}}R$, will reduce $k$(calc) from nearly 2 to zero; and a relative accuracy of one percent is considered reasonably good for reflectance measurement (Piller and von Gehlen, 1964, p. 872). Even smaller errors in both $R$ and ${}^{\mathrm{im}}R$, of the same signs as before, will give an imaginary point; thus (+)0.15 percent in $R$ together with (−)0.3 percent in ${}^{\mathrm{im}}R$, both relative, lead to values of 7.001 for $n$(calc) and 1.661$i$ for $k$(calc).

*Limiting values of n and k*

For any measured value of reflectance, air or oil, there are maximum and minimum values of both $n$ and $k$ that are compatible with that reflectance, and these are defined by the geometry of the reflectance curve (Fig. 1). The maximum value of $n$ is obtained from (1) or (2) when $k = 0$; it may readily be shown that $n_{\max}$ (oil) $= N(1 + \sqrt{{}^{\mathrm{im}}R})/(1 - \sqrt{{}^{\mathrm{im}}R})$, and that $n_{\max} \cdot n_{\min} = N^2$, with corresponding relations for air reflectances. The maximum value of $k$ is at the top of the semicircular reflectance curve, and is equal to the length of the radius [equation (4)]; $k_{\min}$, of course, is zero.

Cervelle *et al.* (1975) have used two-media reflectances to obtain $n$ for sphalerite, and have recommended the method as generally applicable to minerals of low absorption provided that Koenigsberger's equation (5) is used for the calculation. This recommendation requires qualification, because errors in oil reflectances are likely to be larger than those in air and the combined effect can be very large. The Koenigsberger equation may be used with caution when the reflectances lead to a real point and the calculated refractive index is not much greater than 3, but it must never be used when the point is in the imaginary field because of the very rapid increase in $n$(calc) beyond the boundary. In such cases a weighted mean between the values of $n_{\max}$ for air and oil will give a much closer approximation to a probable true value.

A minimum value of the absorption index (kappa), below which a mineral may be considered transparent in thin section, was calculated by Wright (1919). If we repeat the calculation for the absorption coefficient (kay), and the standard value of 0.03 mm for the thickness of a modern thin section, we obtain values of $k$ of about 0.015 at 400 nm and 0.026 at 700 nm. Merwin (1915) used immersion methods to measure the refractive index of covelline, for which the minimum absorption coefficient is near 0.3, but only succeeded because the cleavage flakes that he used were extremely thin.

*Smoothing techniques*

Many authors have used a smoothing technique to obtain low values of $k$, by making adjustments to experimental dispersion curves for reflectance until the dispersion curves for $n$ and $k$ are also smooth. Vierne and Brunel (1977) have shown that smooth dispersion curves for reflectance must lead to smooth curves for the two optical constants, but it does not follow that low values of $k$ (nor high values of $n$) obtained in this way are necessarily reliable unless the

intersection angles are favourably large. When the reflectances give points near the $k = 0$ boundary, equally probable smooth curves can be obtained for a wide range of values of $n$(calc) and especially of $k$(calc).

## Discussion

Two general statements on the two-media method by previous authors are worth quoting. Von Gehlen and Piller (1965) said: "Although the errors of $n$ and $k$ vary widely, depending on their absolute values, it is often possible to calculate $n$ and $k$ with reasonable accuracy" (p. 335), and "Generally, our experience is that the relative errors of reflectivity measurements are much larger than normally accepted, even under favourable circumstances, although sometimes the 'reproducibility' of a single set-up may be rather good. But this does not give the real error" (p. 340). F. E. Wright (1919, p. 446), on the other hand, was more pessimistic: "The above equations show that it is in general not possible to measure both the refractive indices and the absorption indices of an opaque body by means of the phenomena resulting on the reflection of vertically incident light waves."

Instruments, and particularly microphotometers, have been greatly improved since Wright's day, but his remarks remain broadly true. The largest obstacle to accurate microphotometry is the absence of a good range of primary reflectance standards. In Figure 6 we have shown that more than half of a large sample of measurements lie within one percent of the oil reflectance value at the boundary of the imaginary field, a region in which the derived constants, especially $k$, are extremely sensitive to measurement errors. Better oil standards will extend the range of reflectance values for which the constants may confidently be derived, but there must remain many substances for which no conceivable improvement in the accuracy of measurement can produce reliable derived constants by the two-media method. We believe that our recommendations for the calculation of results will enable other workers readily to distinguish between feasible and practically impossible cases. Despite our analysis, we feel strongly that the two-media method has much to offer in favourable circumstances, and that even when the absorption is too small to be derived there is considerable scope for refractive index and dispersion determination on transparent and translucent minerals.

## Appendix

We have recommended the use of the $n/k$ diagram with intersection angle contours (Fig. 2), and the $R/{}^{\text{im}}R$ cigar diagram (Figs. 4 and 6), as adjuncts to the calculation of $n$ and $k$ and the errors in both. The equations for the curves are collected here to avoid cluttering the text; all have been derived from the reflectance equations (1) and (2).

*Intersection angle contours*

Figure 2 was constructed from tabulated values of $\alpha$, $\beta$, and $(\beta - \alpha)$ by interpolation. The explicit equations are not compact.

$$\tan\alpha = 2nk/(n^2 - k^2 - 1)$$
$$\tan\beta = 2nk/(n^2 - k^2 - N^2)$$

The intersection angle may be obtained directly from the measured reflectances; application of the cosine rule leads to the equation

$$\frac{R + {}^{\text{im}}R - 2\sqrt{R \cdot {}^{\text{im}}R} \cdot \cos(\beta - \alpha)}{(1 - R)(1 - {}^{\text{im}}R)} = \frac{(N-1)^2}{4N} \; (= M)$$

which is easily rearranged as required. Solution as a quadratic in $\sqrt{{}^{\text{im}}R}$ enables a contour of constant $(\beta - \alpha)$ to be plotted directly on the $R/{}^{\text{im}}R$ cigar diagram by the equation

$$\sqrt{{}^{\text{im}}R} = \frac{\sqrt{R} \cdot \cos(\beta - \alpha)}{M(1 - R) + 1} \pm \sqrt{\{\text{1st term}\}^2 + \frac{M(1-R) - R}{M(1-R) + 1}}$$

Both equations are symmetrical in $R$ and ${}^{\text{im}}R$, which may thus be substituted for each other. From these reflectance values we can calculate $n$ and $k$ to plot a contour directly on the $n/k$ diagram.

*Constant-k (kay) curves on the cigar diagram*

These equations, derived from equation (6a) in the text, are:

$$h = \frac{a(2k^2 + N^2 + 1)}{2(k^2 + 1)} \pm \frac{(N^2 - 1)}{2(k^2 + 1)}\sqrt{(a^2 - k^2 - 1)}$$

$$a = \frac{h(2k^2 + N^2 + 1)}{2(k^2 + N^2)} \pm \frac{(N^2 - 1)}{2(k^2 + N^2)}\sqrt{(h^2 - k^2 - N^2}$$

where $a$ and $h$ are as given in equation (3) in the text. The explicit equations in $R$ and ${}^{\text{im}}R$ are clumsy.

*Constant-κ (kappa) curves on the cigar diagram*

$$h = \tfrac{1}{2}a(N^2 + 1) \pm \tfrac{1}{2}(N^2 - 1)\sqrt{(a^2 - \kappa^2 - 1)}$$

$$a = \frac{h(N^2 + 1)}{2N^2} \pm \frac{(N^2 - 1)}{2N^2}\sqrt{\{h^2 - N^2(\kappa^2 + 1)\}}$$

The curves of constant absorption index, unlike those for constant absorption coefficient, are symmetrical about the diagonal $R = {}^{\text{im}}R$.

*Constant-n curves on the cigar diagram*

$${}^{\text{im}}R = \frac{\frac{1}{2n}(N^2 - 1) + (a - N)}{\frac{1}{2n}(N^2 - 1) + (a + N)} \quad \text{where } a = \left(\frac{1 + R}{1 - R}\right)$$

We use this form of the equation so that ${}^{\text{im}}R$ is calculable when $n$ is infinite.

In each case where the equations are expressed in $a$ and $h$, we obtain the reflectances from $R = (a - 1)/(a + 1)$ and ${}^{\text{im}}R = (h - N)/(h + N)$.

## Acknowledgments

We thank our colleagues Drs. M. H. Hey, M. Hills, N. F. M. Henry, and Professor T. G. Vallance for their patient advice and encouragement; we do not hold them responsible for our conclusions. We also thank Miss V. Jones, Mr. P. Hicks, and Mr. G. Bearne for help with the diagrams.

## References

Cervelle, B., C. Lévy and M. Pinet (1975) Determination by reflectometry of the refractive indices of sphalerite; experimental accuracy and surface conditions. *Fortschr. Mineral., 52,* 539–548.

Clarke, F. J. J. (1972) High accuracy spectrophotometry at the National Physical Laboratory. *J. Res. Natl. Bur. Stand., 76A,* 375–403.

Coxeter, H. M. S. (1969) *Introduction to Geometry.* Wiley, New York.

Drude, P. (1890) Ueber die Reflexion und Brechung ebener Schallwellen an der Grenze zweier isotroper mit innerer Reibung behafteter Medien. *Annalen Phys. Chem., 61,* 759–769.

Galopin, R. and N. F. M. Henry (1972) *Microscopic Study of Ore Minerals.* Heffer, Cambridge, England.

Gehlen, K. von and H. Piller (1964) Zur Optik von Covellin. *Beitr. Mineral. Petrogr., 10,* 94–110.

——— and ——— (1965) Optics of hexagonal pyrrhotine ($Fe_9S_{10}$). *Mineral. Mag., 35,* 335–346.

Hallimond, A. F. (1970) *The Polarizing Microscope.* Vickers Ltd., Vickers Instruments, York (3rd ed.).

Holl, H. B. (1967) Specular reflection and characteristics of reflected light. *J. Optical Soc. Am., 57,* 683–690.

Koenigsberger, J. (1913) Über Messungen des Reflexionsmögens und Bestimmung der optischen Konstanten. *Annalen Phys., 43,* 1205–1222.

Lopez-Soler, A. and J. M. Bosch-Figueroa (1970) Optical characteristics of enargite. *Trans. Inst. Mining Metallurgy, 79,* B249–B252.

Merwin, H. E. (1915) Covellite: a singular case of chromatic reflection. *J. Wash. Acad. Sci., 5,* 341–344.

Pepperhoff, W. (1965) Quantitative Auflichtmikroskopie mit Hilfe aufgedampfter Interferenzschichten. *Arch. Eisenhüttenwesen, 36,* 941–950.

Piller, H. (1967) Influence of light reflection at the objective in the quantitative measurement of reflectivity with the microscope. *Mineral. Mag., 36,* 242–259.

——— (1974) Modern techniques in reflectance measurements. *J. Microscopy, 100,* 35–48.

——— (1977) *Microscope Photometry.* Springer-Verlag, Berlin.

——— and K. von Gehlen (1964) On errors of reflectivity measurements and of calculations of refractive index $n$ and absorption coefficient $k$. *Am. Mineral., 49,* 867–882.

Ponomareva, M. N. (1958) Problems of the relations between the reflection properties of ore minerals and their structural peculiarities. (in Russian) *Dokl. Akad. Nauk. SSSR, 121,* 162–164.

Vierne, R. and R. Brunel (1977) Constantes optiques de la clausthalite PbSe dans le visible. *Bull. Soc. fr. Mineral. Cristallogr., 100,* 110–113.

Volynskii, I. S. and S. N. Yasnopol'skii (1959) Measurement of the optical constants of ore minerals. II. The determination of $n$ and $k$ of light-absorbing minerals from the measured value of $R$. (in Russian) *Trudy Inst. Miner. Geokhim. Kristallokhim. Redkikh Elementov, 3,* 215–226.

Wright, F. E. (1919) Polarized light in the study of ores and metals. *Proc. Am. Phil. Soc., 58,* 401–447.

*Manuscript received, April 3, 1978; accepted for publication, June 7, 1978.*